NOVEL CONSTANT-FREQUENCY ACCELERATION TECHNIQUE FOR NON-SCALING MUON FFAGS

S. Koscielniak*, TRIUMF, 4004 Wesbrook Mall, Vancouver, B.C., Canada

Abstract

There is a resurgence of interest in Fixed Field Alternating Gradient (FFAG) accelerators, both in traditional "scaling" and in novel "non-scaling" machines. We focus on the linear-field FFAG which offers very high momentum compaction. Muons require fast acceleration to avoid decay losses; this necessitates using superconducting magnets and cavities whose field and frequency are fixed. Fixed-field acceleration implies the orbit and path length unavoidably change with energy; this results in phase slip of particles relative to a fixed-frequency waveform. Nonetheless, depending on the number and location of the fixed points of motion, acceleration is possible for a limited number of turns, during which the beam crosses back and forth the crest. This is facilitated by a serpentine channel extending from injection to extraction energy when a threshold value of voltage is exceeded. Emphasis is given to quadratic dependence of path length on momentum as occurs in the nonscaling muon FFAGs. Finally, mention is made of the relevance of fixed points to longitudinal motion in an imperfectly isochronous cyclotron.

SYNCHRONOUS ACCELERATION

Maintaining *synchronism* between the charged particles and the rf cavity oscillating electric fields is of paramount importance if deceleration is to be avoided. The phase of the accelerating waveform is determined by the frequency and the particle arrival time, which in turn depends on speed and path length. In the isochronous cyclotron, the increasing length of the spiral orbit is adjusted to keep synchronism with the rf field in the dees and the beam rides the crest of the wave; beam delivery is c.w. In the synchrotron, the radio-frequency is swept to match the revolution period of the centroid and the head and tail are periodically interchanged by synchrotron oscillations. In the classical MURA[1] FFAG[1, 2], the central orbit spirals (in a geometrically self-similar fashion) but is not isochronous and so the rf is swept. In distinction to the synchrotron where the repetition rate is limited to of order hertz by the ramping of magnetic fields, the fixed-field accelerator may sweep the rf at repetion rates up to order kilo-hertz and thereby enjoys, in principle, a two orders of magnitude advantage in time-averaged beam current.

Generally, two alternate means of arranging synchronism are used. (I) There is (almost) no net arrival-time variation and acceleration proceeds on-crest, as in the isochronous AVF-cyclotron where spiral path length is adjusted to exactly compensate varying orbit speed. (II) Speed or path-length variation of the beam centroid is compensated by rf sweeping, as in the synchrotron and scaling FFAG respectively. In this second case, the bunch is confined (despite a small spread of momenta and arrival-time deviations from the centroid) by synchrotron oscillations. Both methods have limitations. Developing a magnetic field shape which simultaneously provides isochronous orbits and resonance-free transverse focusing over a large momentum range is (probably) not possible in cyclotrons because tune $\nu_r = \gamma = E/m_0c^2$. The scaling FFAG[1] and synchrotron adopt the approach of constant transerse tunes and non-isochronous orbits. Though it has a large longitudinal acceptance, the transverse acceptance of the former is somewhat limited by the non-linear field profile and resonances. When operated d.c. the synchrotron lattice yields a pitifully small longitudinal acceptance due to chromaticity and horizontal dispersion.

Notice, though strongly influenced by cost and technical difficulty, the matter of c.w. versus pulsed operation is a matter choice; lack of isochronism can be overcome by "brute force" instead of frequency sweeping. If the energy increment per turn is large enough, then it will be possible to achieve the final energy before an accumlated phase slip of $\pi/2$ leads to deceleration.

Almost isochronous FFAG

The linear-field, varying-tune non-scaling FFAG accelerator[3, 4] has recently emerged[7, 9] in the context of fast muon acceleration for a Neutrino Factory and/or Muon Collider[12]. For this application, large 6-dimensional acceptance is required by the diffuse beam from the muon production target; and so short is the muon decay time that the rapid on-crest acceleration is envisaged to take no longer than a few turns. In this extreme regime it is possible for the particle beam in a linear magnetic lattice to cross integer and half-integer transverse resonances without significant degredation.

On the few-turn time scale, the radio frequency cannot be other than fixed; and the machine could in principle be operated c.w. Ideally such a machine would be isochronous, but this is not possible over the $\pm 50\%$ $\Delta p/p$ momentum range intended. The linear dependence of path-length on momentum is set to zero, leaving the second order (quadratic) term to dominate the longitudinal dynamics of this *almost isochronous* FFAG. This leads to an asynchronous-type acceleration in which the beam centroid crosses back and forth and back the crest of the sinusoidal waveform during the transit from injection to extraction.

Asynchronous acceleration is best understood in terms of the longitudinal phase space and its number and nature

*TRIUMF receives federal funding via a contribution agreement through the National Research Council of Canada

[1]The Midwestern Universities Research Association.

of the fixed points of motion. Ilucidating the nature of this motion leads to a general principle for acceleration over a range spanning multiple fixed points: the rf voltage must exceed the critical value to link the unstable fixed points in a zig-zag ladder of straight line segments. The direction of phase slip reverses at each fixed point, and so the criterion is simply that the voltage be large enough that another fixed point be encountered before a π phase slip has accumulated. Beyond the critical voltage value, a serpentine (possibly narrow) channel extending between injection and extraction energy (and back) opens up and the longitudinal acceptance rises from zero. This principle was employed[11] to give analytic criteria for the opening of acceleration channels in systems with parabolic, cubic and quartic dependence of path length on momentum; that is 2, 3 and 4 fixed points, respectively, for each π of rf phase.

QUADRATIC TOF DEPENDENCE

Let the time of flight (ToF) range per cell be ΔT over the energy range ΔE, and the peak energy increment per cell be δE. Let the index n denote iteration number, E_n be the particle energy and t_n, T_n be the absolute and relative arrival times, respectively. Let τ_0 be the cell traversal time at the reference energy E_r. Then $t_n = T_n + n\tau_0$. The longitudinal motion in the linear-field FFAG accelerator may be modelled by the following difference equations:

$$E_{n+1} = E_n + \delta E \cos(\omega T_n) \quad (1)$$

$$T_{n+1} = T_n + 4(E_{n+1} - \bar{E})^2 \Delta T/\Delta E^2 - \delta T_2 \ . \quad (2)$$

Here $\bar{E} = (\hat{E} + \check{E})/2$, $\Delta E = \hat{E} - \check{E}$ and $\Delta T = \delta T_1 + \delta T_2$. The time slip δT_2 represents the fact that the radio-frequency is synchronous with the orbital period at E_r, which is not ncessarily equal to the mean energy $\bar{E}$. These equations have served as a basis for analytic and numerical studies for some time[5, 6]. Supplementary equations to describe effects of beam loading of the rf cavity have been introduced[10], but are not considered here.

We introduce dimensionless variables: $x = \omega T$ and $y = (E - \bar{E})/\Delta E$; and dimensionless parameters: $s \equiv n\omega\Delta T$, $a \equiv (\delta E/\Delta E)/(\omega\Delta T)$, $b \equiv (\delta T_2/\Delta T)$; and approximate the motion by differential equations:

$$x' \equiv dx/ds = (2y)^2 - b \ \text{ and } \ y' \equiv dy/ds = a\cos x \ . \quad (3)$$

The injection and extraction energies $\check{E}, \hat{E}$ correspond to $y = \mp 1/2$, respectively. The reference energy is the solution of $T_{n+1} = T_n$, namely $E_r = \bar{E} \pm (\Delta E/2)\sqrt{b}$ where the ratio b may take any value between 0 and 1.

Choice of operating point

The doublet (a, b) is the key parameter of the system. In general, the choice of operating point will depend not only on acceleration range ($\check{y}$ to $\hat{y}$) and acceptance, but also up on a compromise between dwell time, acceleration efficiency, and dispersion of arrival time (which leads to nonlinear emittance distortion). Matching of the input beam depends also on (a, b).

The half-period τ, the dwell time from low to high momentum is of significance - particularly for decay losses.

$$\tau = \int ds = \int_{\check{x}}^{\hat{x}} dx/x' = \int_{\check{y}}^{\hat{y}} dy/y' \ . \quad (4)$$

The average value of $\cos x$ along the path indicates the efficiency of acceleration and is also of interest: $\langle \cos x \rangle a\tau = (\hat{y} - \check{y})$. The dispersion in dwell times, for particles with differing values c of the hamiltonian, is measured by the normalized second derivative $C_2 \equiv (\partial^2\tau/\partial c^2)/\tau/2$ evaluated at $c = 0$. The significance of C_2 is that it leads, after acceleration, to a spread in x, y values and so it must be minimized. For brevity, let $\mathbf{x} = (x, y)$.

The observation that the incremental dwell time is proportional to the square of the increment c, that is $\tau(a, c) = \tau(a, 0)[1 + C_2c^2 + \ldots]$, is key to minimizing bunch distortion. The phase space about the reference particle must be loaded in such away that $|c|$ takes (almost) the same value at all points on the perimeter of the ensemble. The optimum aspect ratio and orientation angle for the phase space ellipse depends on (a, b) and the centroid $\mathbf{x}_0$, and must match to the injected beam values.

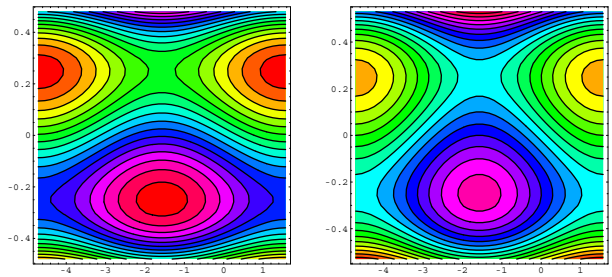

Figure 1: Phase space of quadratic pendulum: $b = 1/4$, $a = 1/48$ (left) and $a = 1/24$ (right).

Hamiltonian and manifolds

Equations (3) above may be derived from the hamiltonian.

$$H(x, y, a, b) = (4/3)y^3 - yb - a\sin x \ . \quad (5)$$

Let c be some particular value of the hamiltonian. Depending on (a, b, c) there are possibly two stable (libration) and three unstable (rotation) manifolds[2] for each 2π range of x. In the former, motion is coperiodic in x and y; and in the latter motion is periodic only in y, and x is unbounded. We are interested in one of the three rotation manifolds. For large momentum offset, there is no possibility of synchronism with the RF and the motion is uni-polar in the ordinate y. However, depending on (a, b, c) there is a serpentine channel in which the rotation is bi-polar in y; and this manifold may be used for acceleration between $\mathbf{x} = \pm(\pi/2, 1/2)$. The realisation[8, 11] that this channel does not open until a minimum critical value of a is exceded is essential to understanding the nonscaling FFAG.

[2] Small angle motion of a pendulum is an example of the first, whereas more than 360° rotation of the pendulum is an example of the second. It is worth noting that *libration* takes its root from the latin libra, for 'scales', and not from the french libré for 'free'.

The motion is synchronous at the two momenta $\pm y_s$, $y_s \equiv \sqrt{b}/2$; and the direction of phase slip reverses above/below these values. This is advantageous because it allows the beam to cross the waveform crest three times before the phase slips to values where it is decelerated.

In each interval $\Delta x = \pi$ there are two elliptic $\mathbf{x}_{1,2} = \pm(\pi/2, +y_s)$ and two hyperbolic $\mathbf{x}_{3,4} = \pm(\pi/2, -y_s)$ fixed points[3]. When $b = 0$, the four fixed points collapse to two. The condition to link the unstable fixed points by a straight line segment with linear acceleration is $H(\mathbf{x}_3) = H(\mathbf{x}_4)$ with solution $a = (1/3)b^{3/2}$; this is the critical value of a for opening of the serpentine channel and it is denoted by the symbol a_c.

The value of the hamiltonian at the unstable fixed points determines the separatrix for the serpentine channel; the value is $H = \pm(a - b^{3/2}/3)\ \forall b$. Hence for bi-polar motion $|c|$ must be smaller than this amount. The *central trajectory* passing through $\mathbf{x} = (0, 0)$ for $c = 0$ has special significance. It gives both the range and minimizes the dwell time; it is the reference path for asynchronous acceleration.

Explicit solutions

Let the cube roots of -1 be: $r_1 = -1$, $r_2 = e^{+i\pi/3}$ and $r_3 = e^{-i\pi/3}$. A trajectory is a contour of constant hamiltonian $H(x, y) = c$, with solutions $y(x)$ given by:

$$y_i = -[r_i w + b/(r_i w)]/2\ , \qquad i = 1, 2, 3 \tag{6}$$

$$w = 3^{1/3}[(c + a\sin x) + \sqrt{(c + a\sin x)^2 - b^3/9}]^{1/3}. \tag{7}$$

Here y_1 is the upper, y_2 is the middle, and y_3 is the lower segment. How many of these solutions we shall need depends on the values of a, b, c and the ranges of x. For a *centre range* of x, momentum y is triple valued and all y_i, are needed; and for *end ranges* either y_1 or y_3 is suitable. The ranges are divided by the turning points $(\check{x}, \hat{x})$ of the motion y_2, namely $\check{x} = -\arcsin[(a_c + c)/a]$ and $\hat{x} = \arcsin[(a_c - c)/a]$ with $a_c = b^{3/2}/3$.

No slip reversal, case of b=0

Setting $b = 0$ is a means to reducing the time dispersion; in this case there is no reversal of the x' slip direction. The range of the channel is given by that of the central trajectory, for which $c = 0$. The width of the channel depends on paths terminating on the fixed points for which $c = \pm a$. The acceleration range extends between $y = \pm\hat{y}$ where $\hat{y} = (3a/4)^{1/3}$. At $x = \pm\pi/2$, the momentum width of the channel is $\delta y = (3a/2)^{1/3}$ – but the useful width is less.

Half period, efficiency and dispersion The period and expectation values will vary with the range over which they are evaluated. Let us first form the values on the fixed range $x = \pm\pi/2$, which implies a varying momentum range $y = \pm(3a/4)^{1/3}$.

For the central trajectory the total dwell time is

$$\tau_u(a, 0) = \sqrt{\pi}\ \Gamma(1/6)/[(6a)^{2/3}\Gamma(2/3)]\ . \tag{8}$$

[3]In assigning coordinates to indices, we take the positive sign first.

On the same trajectory, the acceleration efficiency is found to be independent of a.

$$\langle\cos x\rangle = 2(3a/4)^{1/3}/[a\tau] \approx 0.823503 \tag{9}$$

In order to find the time dispersion, we must compute the half period for motions off the central trajectory. The lowest order terms in a Taylor series about $c = 0$ are *exactly*

$$\frac{\tau_u(a, c)}{\tau_u(a, 0)} = \left[1 + \frac{2}{9}\left(\frac{c}{a}\right)^2 + \frac{32}{243}\left(\frac{c}{a}\right)^4 + \frac{3136}{32805}\left(\frac{c}{a}\right)^6 \ldots\right] \tag{10}$$

We have not yet considered whether these paths cross the nominal acceleration range $y = \pm 1/2$. This first occurs when $a = 1/6$ and the x-range extends between $\pm\pi/2$. For larger values of a, the range of x for which $|y| \le 1/2$ is smaller and we must reduce the corresponding ranges of integration to $x = \pm\arcsin[1/(6a)]$. We refer to the dwell time between these points as the *restricted period* τ_r:

$$\tau_r(a, 0) = \frac{1}{a}\mathcal{F}_{21}\left[\frac{1}{6}, \frac{1}{2}, \frac{7}{6}, \frac{1}{(6a)^2}\right]\ . \tag{11}$$

Here $\mathcal{F}_{21}$ is the hypergeometric function. We may also obtain the average value of cosine over the interval $\hat{y} - \check{y} = 1$, i.e. $\langle\cos x\rangle_r = 1/[a\,\tau_r] = 1/\mathcal{F}_{21}[\ldots]$. This quickly approaches unity for $a > 1/4$.

The dwell time for paths with $c \neq 0$ can be computed. The expressions are lengthy; we present one special case.

$$\begin{aligned} \tau_r(1/6, c) &= \tau_r(1/6, 0)\left[1 + 8c^2 + (512/3)c^4 + \ldots\right] \\ \tau_r(1/6, 0) &= \sqrt{\pi}\ \Gamma(1/6)/\Gamma(2/3) \approx 7.28595 \end{aligned} \tag{12}$$

In general derivative C_2 falls rapidly as a increases.

Two slip reversals, case $b \neq 0$

The working is facilitated by writing the solutions in the form $y(x(z))$ where the relation between x, z depends on the range of x, as given in the table below.

x range	transformation	z range
$\hat{x} \to +\pi/2$	$(c + a\sin x) = +a_c\cosh z$	$0 \to \hat{z}$
$\check{x} \to \hat{x}$	$(c + a\sin x) = a_c\sin z$	$\mp\pi/2$
$-\pi/2 \to \check{x}$	$(c + a\sin x) = -a_c\cosh z$	$\check{z} \to 0$

Here $a_c = b^{3/2}/3$ and $\check{z} = -\text{arccosh}[(a - c)/a_c]$, $\hat{z} = +\text{arccosh}[(a + c)/a_c]$. Over the end ranges $z = [\check{z}, 0]$ and $z = [0, \hat{z}]$, the two solutions become $y_1 = -y_3 = +\sqrt{b}\cosh(z/3)$, and the speed is given by $v_1 = v_3 = b[1 + 2\cosh(z/3)]$. Over the centre range $z = \mp\pi/2$ the three solutions become

$$y_1 = +\sqrt{b}\cos[(z - \pi/2)/3] \tag{13}$$

$$y_2 = -\sqrt{b}\sin[z/3] \tag{14}$$

$$y_3 = -\sqrt{b}\cos[(z + \pi/2)/3]\ , \tag{15}$$

and the speed $v \equiv (2y)^2 - b$ is given by

$$v_1/b = 1 + 2\cos[(2z - \pi)/3] \tag{16}$$

$$v_2/b = 1 - 2\cos[2z/3] \tag{17}$$

$$v_3/b = 1 + 2\cos[(2z + \pi)/3]\ . \tag{18}$$

The connection between z and time-like s is the dwell time, introduced in (4) and elaborated in (21). In general the integral cannot be found in closed form, nor can it be inverted for $z(s)$. However, for the special case of $a = a_c$ and $c = 0$, the relation may be constructed piecewise for y_i thus: $\tanh[s_{1,3}b/\sqrt{3}] = \tan[(z \pm \pi/2)/3]/\sqrt{3}$, $\tanh[-s_2 b/\sqrt{3}] = \tan[z/3]/\sqrt{3}$.

Range and width of channel The range of the serpentine channel is found by substituting $x = \pm\pi/2$ in the central trajectory $y(x, c = 0)$. The range extends between

$$\pm y = \sqrt{b}\cosh[(1/3)\text{arccosh}(a/a_c)] \ . \qquad (19)$$

At the critical value a_c the range spans $y(a_c) = \pm\sqrt{b}$.

The paths emanating from the unstable fixed points constitute the separatrix and define the momentum width at $x = \pm\pi/2$. Substituting values of the hamiltonian at these points into $y_1(x, c)$, we find the lower and upper bounds to be respectively $y = \sqrt{b}$ and

$$y = \sqrt{b}\cosh[(1/3)\text{arccosh}(2a/a_c\ - 1)] \ . \qquad (20)$$

Channel width rises as b falls, but collapses when $a = a_c$.

Half period, efficiency and dispersion In general, expressions for dwell time, acceleration efficiency and time dispersion cannot be obtained in closed form, and numerical methods must be resorted to. However, there are interesting and useful special cases.

Mathematically the simplest case is that the integration ranges are $y = \pm\sqrt{b}$, or $x = \pm\arcsin(a_c/a)$, or $z = \pm\pi/2$. For hamiltonian value c, the dwell time is

$$\begin{aligned}\tau &= \int_{\check{x}(c)}^{\hat{x}(c)} \frac{dx}{v(x,c)} = \int_{-\pi/2}^{+\pi/2} \frac{dz}{v(z,c)}\left(\frac{dx}{dz}\right) \qquad (21)\\ &= \frac{b^{3/2}}{3a}\int_{-\pi/2}^{+\pi/2}\frac{dz}{v(z)}\frac{\cos z}{\cos x} = 2\frac{\sqrt{b}}{3a}\int_{-\pi/2}^{+\pi/2} dz \frac{\cos(z/3)}{\cos x(z)} \ .\end{aligned}$$

When $c = 0$ the integral is obtained (almost) exactly:

$$\tau(a, 0) = 4\sqrt{b}/(a\pi)\mathcal{K}[(a_c/a)^2] \ . \qquad (22)$$

The series expansion for $\mathcal{K}$, the complete elliptic integral of the first kind, converges quickly for $b^{3/2} < a$. On the central trajectory, the acceleration efficiency is

$$\langle\cos x\rangle = 2\sqrt{b}/[a\tau] = (\pi/2)/\mathcal{K}[\ldots] \ , \qquad (23)$$

which tends very quickly to unity because x' is smallest in around the crest and largest near the zero crossing.

To find the dispersion we must find the dwell time for paths with $c \neq 0$, namely $\tau(a, c) \approx \tau(a, 0) +$

$$+\frac{2\sqrt{b}\,c^2}{a(a^2 - a_c^2)^2}\left(2a^2\mathcal{E}[\ldots] + (a_c^2 - a^2)\mathcal{K}[\ldots]\right) + \ldots \qquad (24)$$

Here $\mathcal{E}$, the complete elliptic integral of the second kind, has argument $(a_c/a)^2$. The dispersion C_2 is essentially the coefficient of c^2 in the Taylor expansion about $c = 0$. A significant feature of the expansion is the resonant denominator terms $(a^2 - a_c^2)$. These occur because, for given a value, the larger is b so the motion is closer to a fixed point; and so we should expect the dispersion in arrival times to increase with b.

Inevitably, attempts have been made to reduce the time dispersion by flat-topping of the rf waveform using second through fifth harmonic. This leads to modified values[11] of the channel range, width and critical parameter a_c.

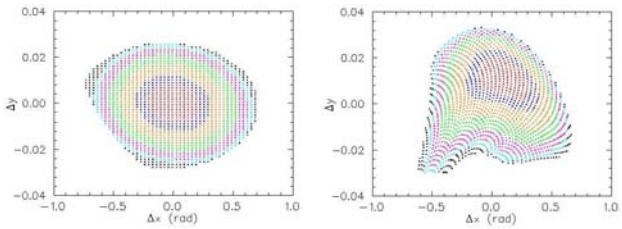

Figure 2: Input (left) and output (right) phase space. $(a, b) = (1/12, 1/6)$, tracking range $x = \pm\pi/2$. Survival is 91.1% based on cuts of $\pm 8\%$ at $\hat{E}$.

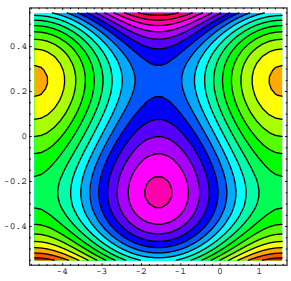

Figure 3: Quadratic pendulum, $(a, b) = (1/12, 1/4)$.

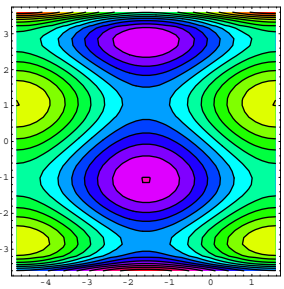

Figure 4: Phase space of quartic pendulum, $\alpha = 1/3$

Choice of operating point

Corresponding to the extraction/injection momenta $y = \pm 1/2$ is the position range $x = \pm\arcsin[(1 - 3b)/(6a)]$; and to $y = \pm\sqrt{b}$ is $x = \pm\arcsin(a_c/a)$. These ranges become identical when $b = 1/4$. In this case, the dwell time, efficiency and dispersion over the restricted range are given by (22,23,24) $\forall a$. Of course, to obtain expectation values over the range $x = \pm\pi/2$, one must integrate also over the *end ranges*; but the contributions are usually small unless $a \gg b$. The restricted range extends to $\pm\pi/2$ when $a = (1 - 3b)/6$; this cannot be satisfied for $a > 1/6$.

The unique values which simultaneously satisfies the channel opening condition $a = (1/3)b^{3/2}$ and the restricted range condition $a = (1 - 3b)/6$ are $(a, b) = (1/24, 1/4)$. This forms a starting point from which to set suitable acceleration parameters. In practise we need a channel of finite width, which implies $a > 1/24$; and the desire to optimise acceptance and dispersion suggests a lowering of b. In the proposed muon FFAGs, the acceleration rate is limited to $a \leq 1/12$ for technical reasons – though this could be raised by reducing the bend per cell. The choice $b = 0$ is ruled out since the acceleration range is inadequate until $a \geq 1/6$. The central trajectory spans

exactly $\mathbf{x} = \pm(\pi/2, 1/2)$ for $(a, b) = (1/12, 1/6)$ and it is anticipated that the optimum operating point is in the vicinity of these values. As example, figure 2 shows the result of particle tracking a 0.5 eV.s phase-space ellipse over 7.5 turns for a 10-20 GeV muon FFAG with 90 cells.

QUARTIC, ETC, PATH DEPENDENCE

Let $y \propto (E - \bar{E})$. Consider the model equations:

$$dx/ds = y^2(1 - \alpha^2 y^2) - 1 \;\text{ and }\; dy/ds = \lambda \cos x \; . \quad (25)$$

This is a complicated system with two free parameters and eight fixed points [$\mathbf{x}_{1,2,3,4} = \pm(\pi/2, p), \pm(\pi/2, -q)$ and $\mathbf{x}_{5,6,7,8} = \pm(\pi/2, -p), \pm(\pi/2, q)$]. For brevity we restrict the discussion. Solutions of $x' = 0$ are the synchronous momenta; values are $y_s = \pm p, \pm q$ with $q > p > 0$:

$$p = \sqrt{2}/\sqrt{1 + w} \; , \quad q = \sqrt{2}/\sqrt{1 - w} \; , \quad w = \sqrt{1 - 4\alpha^2} \; .$$

The critical value λ for which a channel encloses the inner, stable fixed points $\pm(\pi/2, p)$ increases with α. There are solutions for the condition to link the unstable fixed points $\pm(\pi/2, -p)$ over the range $\alpha = [0, 1/2]$ and end-point values are $\lambda = 2/3$ and $\lambda = 8\sqrt{2}/15$. For larger values of λ the channel attains a finite width.

The condition, $H(\mathbf{x}_5) = H(\mathbf{x}_6) = H(\mathbf{x}_7) = H(\mathbf{x}_8)$, to link all the unstable fixed points in a ladder has a unique solution: $\alpha = 1/3$, $\lambda_c = 2\sqrt{3}/5 \approx 0.69282$. In this case $q, p = \sqrt{3(3 \pm \sqrt{5})/2} \approx 2.80, 1.07$ and a bi-serpentine channel emerges with twice as many meanders as in the quadratic case. The beamlet is accelerated between $\mathbf{x} = \pm(\pi/2, -2\sqrt{3})$. Four reversals of phase slip is seen as advantageous; because it allows the beamlet to cross the crest of the waveform five times before the beam slips to values where deceleration occurs. If λ is increased well beyond the critical value; then the channel appears almost vertical.

AVF Cyclotron

The quartic system yields an acceleration channel which begins to be reminiscent of that seen in experimental measurements of the phase histories versus energy (or radius) of accelerating and decelerating beams in the TRIUMF cyclotron[13]. Based on that observation, Baartman[14] proposed that the phase wiggles owe their existence to a ladder of fixed points. (If the machine were perfectly isochronous, the paths would be vertical with no wiggles.) Calculations by Rao[14] verified this proposition and suggests there to be at least eight fixed points in the ladder. Thus, the asynchronous acceleration principle devised to predict the properties of the linear-field non-scaling FFAG is seen to be perfectly at home in the world of (nearly) isochronous cyclotrons where there is the relative freedom to adjust the magnet lattice and field profile by shims and correction coils and thereby produce a relative time of flight variation that is characterised by a high order polynomial.

Fig. 5 was generated with the computer program COMA, using transfer matrices computed by CYCLOP from a magnet field model of the TRIUMF cyclotron that is a composite of the basic measured field, measured coil contributions and a mathematical adjustment of the coil currents to make the computer model accelerate beam to 500 MeV in the machine midplane. The D-voltage is 91 kV, and the wave crest is at 90°. Particle initial energies were arranged between 50 and 500 MeV, while the starting RF phase angle was adjusted artificially in order to get nice looking islands and a separatrix. Although Fig. 5 is a calculation, the coarser features have been experimentally verified[13].

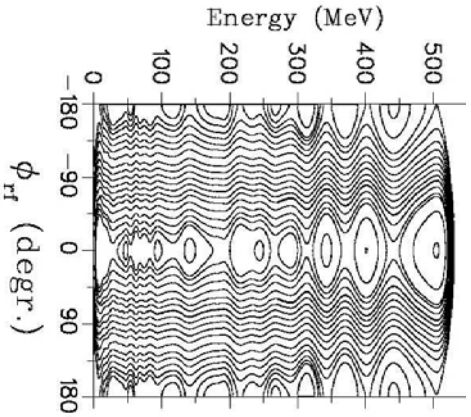

Figure 5: Phase history for TRIUMF cyclotron

Acknowledgements

Many people, in particular S.J. Berg, M. Blaskiwicz, E. Courant, A. Garren, E. Keil, S. Machida, F. Mills, Y. Mori, R. Palmer, A. Sessler and D. Trbojevic, have contributed novel, frontier ideas, and the present author has benefitted greatly from discussions with these colleagues. The author wishes also to thank particularly collaborators Carol Johnstone (FNAL) and Michael Craddock (TRIUMF-UBC).

REFERENCES

[1] F.T. Cole: Proc. 2nd Int. Conf. on High Energy Accelerators, CERN Geneva Switzerland, 1959, pg. 82.

[2] F.T. Cole: Proc. 3rd Int. Conf. on High Energy Acceleators, BNL Upton, N.Y. USA, 1961, pg. 317.

[3] Johnstone: Proc. 4^{th} Int. Conf. Physics Potential & Development of $\mu^+\mu^-$ Colliders, San Fran., Ca., Dec. 1997, 696-698.

[4] C. Johnstone *et al*: Proc. 1999 Particle Accelerator Conf. New York City N.Y., 29-March - 02-April 1999, pg. 3068.

[5] C. Johnstone and S. Koscielniak: Proc. Snowmass 2001 Meeting, SLAC-R-599, eConfC010630, T508.

[6] J.S. Berg: *ibid*, T503.

[7] J.S. Berg *et al*: Proc. 2003 Particle Accelerator Conf., Portland Or., May 12-16 2003, pg. 3413.

[8] S. Koscielniak & C. Johnstone: *ibid*, pg. 1831.

[9] E. Keil & A. Sessler: *ibid*, pg. 414.

[10] D. Trbojevic & M. Blaskiewicz: FFAG Workshop, LBNL, Nov. 2002, http://www.cap.bnl.gov/mumu/conf/ffag-021028.

[11] S. Koscielniak & C. Johnstone: Nuclear Instruments & Methods-A **523**. pgs. 25-49, May 2004.

[12] The Neutrino Factory and Muon Collier Collaboration: http://www.cap.bnl.gov/mumu/

[13] M. Craddock *et al*: IEEE Trans. Nuc. Sci. Vol. NS-24, No.3, June 1977, p.1615.

[14] R. Baartman and Yi-Nong Rao: personal communication, TRIUMF, Vancouver B.C., 2004.